

# RSC Advances



This is an *Accepted Manuscript*, which has been through the Royal Society of Chemistry peer review process and has been accepted for publication.

*Accepted Manuscripts* are published online shortly after acceptance, before technical editing, formatting and proof reading. Using this free service, authors can make their results available to the community, in citable form, before we publish the edited article. This *Accepted Manuscript* will be replaced by the edited, formatted and paginated article as soon as this is available.

You can find more information about *Accepted Manuscripts* in the [Information for Authors](#).

Please note that technical editing may introduce minor changes to the text and/or graphics, which may alter content. The journal's standard [Terms & Conditions](#) and the [Ethical guidelines](#) still apply. In no event shall the Royal Society of Chemistry be held responsible for any errors or omissions in this *Accepted Manuscript* or any consequences arising from the use of any information it contains.



## ARTICLE

## Influence of Photoactivated Tetra Sulphonatophenyl Porphyrin and TiO<sub>2</sub> nanowhiskers on Rheumatoid Arthritis infected Bone Marrow Stem Cells proliferation *in vitro* and oxidative stress biomarkers *in vivo*

Received 00th January 20xx,  
Accepted 00th January 20xx

DOI: 10.1039/x0xx00000x

www.rsc.org/

Fawad Ur Rehman,<sup>a</sup> Chunqiu Zhao,<sup>a</sup> Changyu Wu,<sup>a</sup> Hui Jiang,<sup>a</sup> Matthias Selke,<sup>b</sup>  
Xuemei Wang<sup>a\*</sup>

Photodynamic therapy (PDT) is mostly used to induce apoptosis or necrosis in the benign and malignant tumors, along with other microbial infections and suppression of autoimmune diseases including rheumatoid arthritis (RA). The bone marrow stem (BMS) cells are also in focus in translational medicine, tissue engineering and as an autoimmune diseases suppressant. In this study we used Tetra Sulphonatophenyl Porphyrin (TSPP) with TiO<sub>2</sub> nanowhiskers for RA PDT and evaluated their effect on stress biomarkers (CAT, SOD, GPX, GR, TAO and MDA) *in vivo* and BMS cells proliferation *in vitro*. We compared four murine groups, three of which had Collagen Induced Arthritis as TP-L (illuminated), TP-nL (dark) and CIA (control), whereas the other group was normal without disease and treatment. All anti-oxidative enzymes and biomarkers were significantly ( $p < 0.01$ ) affected by the treatment except TAO ( $p > 0.05$ ). Moreover, we also evaluated the growth proliferating effect of TSPP-TiO<sub>2</sub> (TP) PDT on the *in vitro* RA infected BMS cells i.e. 25  $\mu$ l had highest cell count ( $12.33 \times 10^6$  cells/well) and 33% more growth rate in photoactivated TP when compared with 50 and 100  $\mu$ l treatment groups. Herein, we report that photoactivated TSPP-TiO<sub>2</sub> for RA PDT may be safer than photosensitizers without the titanium nanomaterials in terms of reduced oxidative stress and also promotion of RA BMS cells growth *in vitro* as novel finding.

### Introduction

Stem cells are specialized, immature cells with prolonged capacity of self-renewal and plasticity to various specialized cell types, i.e., osteoblast, chondrocytes, adipocytes, neurons, myocytes under certain favorable conditions or differentiation medium<sup>1, 2</sup>. Almost all the vital organs and tissues in the body contain stem cells. The Bone Marrow Stromal or Stem (BMS) cells are named after their origin, i.e., from the bone marrow of long bones, which was first time reported by Friednstein et al<sup>3</sup>. BMS cells are colonogenic and have the potential to proliferate ex

*vivo* without any structure or functional deformation and differentiate to various types of specialized cells<sup>4</sup>. On the bases of these vital properties BMS cells have been explored for potential cure of various maladies<sup>5</sup>, cancers<sup>6</sup>, tissue engineering<sup>7</sup> and autoimmune diseases; notably rheumatoid arthritis (RA)<sup>8, 9</sup>.

RA is an autoimmune progressive joint inflammatory disease in humans with unknown etiology<sup>10</sup>. So far, multiple triggers have been attributed to the onset of RA, e.g., age, gender, lifestyle, and genetic makeup of the individual<sup>11</sup>. The worst feature of RA is persistent chronic inflammation that leads to 50-70 % disability in the patients in 10-15 years<sup>12</sup>. TNF- $\alpha$  is the most commonly investigated biomarker for RA and considered as key proinflammatory cytokine in RA synovial milieu<sup>13</sup>. To date, only empirical therapy is commonly employed to suppress the clinical signs in RA patients and no proper treatment is available<sup>14</sup>.

<sup>a</sup> State key Laboratory of Bioelectronics, School of Biological Science and Medical Engineering, Southeast University, Sipailou 2, Nanjing 210096, Jiangsu China

<sup>b</sup> Department of Chemistry and Biochemistry, California State University, Los Angeles, CA 90032, USA

E-mail: xuewang@seu.edu.cn

Photodynamic therapy (PDT) is therapeutic procedure which consists of Photosensitizer (PS), visible light and biologically available oxygen<sup>15</sup>. Porphyrin derivatives are the most popular PS for cancers and infectious diseases<sup>16</sup>, despite adverse effects including accumulation of the PS in vital organs, neurotoxicity and phototoxicity. These adverse effects have limited biomedical applications of the porphyrin derivatives<sup>17, 18</sup>. PDT has been reported as a successful remedy for various neoplastic and non-neoplastic maladies<sup>19</sup>. When the PS is photoactivated with visible light it will generate singlet oxygen ( $^1\text{O}_2$ )<sup>20</sup> as the main cytotoxic agent, although other ROS such as hydroxyl radical and other radicals are also produced. These ROS and  $^1\text{O}_2$  will interact with cellular signaling pathways and induce apoptosis or necrosis<sup>21</sup>. However, the intracellular antioxidant enzyme systems will be activated to neutralize these ROS and protect the cells from injury<sup>21</sup>. Superoxide dismutase (SOD), Glutathione Peroxidase (GPX), and Glutathione reductase (GR) are among the vital anti-oxidative enzymes as ROS scavengers while Malondialdehyde (MDA) is an oxidative stress biomarker<sup>22</sup>.

Titanium is second most abundantly used nanomaterial for human consumption; either as a food additive, environmental scavenger, in sunscreens and also in various biomedical applications<sup>23</sup>. In biomedical applications it is commonly used in prosthetic orthopedic implants, nano drug delivery systems, sonodynamic therapy, and photodynamic therapy<sup>24</sup>. Nano Titanium dioxide ( $\text{TiO}_2$ ) became popular for cancer theranostics after the first introduction by Fujishima et al almost two decades ago<sup>25</sup>. The use of  $\text{TiO}_2$  nanowhiskers for cancer therapy was already reported by Li et al<sup>26</sup>. And the biomedical applications of  $\text{TiO}_2$  nanowhiskers combined with TSPP were also reported recently, which demonstrated higher efficacy of Tetra Sulphonatophenyl Porphyrin (TSPP) combined with  $\text{TiO}_2$  nanowhiskers during RA PDT as compared to TSPP and  $\text{TiO}_2$  alone<sup>27</sup>. It is observed that the TSPP- $\text{TiO}_2$  nanocomposites had excellent theranostics effect by successfully lowering the TNF- $\alpha$  and IL-17, i.e., major proinflammatory factors and biomarkers for RA and bio-imaging the subclinical RA that was confirmed at the onset of clinical signs. Similarly, the TSPP- $\text{TiO}_2$  nanocomposites had protective effect on circulatory and excretory system in murine models by lowering the relevant liver (i.e. AST, ALT and LDH) and kidneys (i.e. BUN and CRT) functional biomarkers in comparison to TSPP and  $\text{TiO}_2$  alone during PDT<sup>28</sup>.

Therefore, considering the above observations and the importance of the cellular antioxidant enzyme systems herein, we report for the first time, the effect of TSPP- $\text{TiO}_2$  on isolated RA BMS cells and various stress enzymes during PDT *in vivo* in murine models.

## Materials and methods

### Chemicals and Animal selection

Male Sprague-Dawley (SD) rats were selected due to their ability to produce excellent model of Collagen induced arthritis (CIA). All the animals were provided standard pallet feed and water ad-libitum with a 12/24 hours daily light cycle. At the beginning of the experiments the average animal weight was  $220 \pm 20$  grams and eight weeks of age. All the experiments involving animals were conducted under the guidelines of Animal Research Ethics Board of Southeast University and were approved by the National Institute of Biological Science and Animal Care Research Advisory Committee of Southeast University, Nanjing, China. All chemicals used in cell culture experiments were purchased from HyClone Laboratories, Inc. Utah, USA, whereas the Collagen type II and Adjuvant were obtained from Chondrex, Inc. The chemicals used for differentiation medium, i.e.,  $\beta$ -Glycerophosphate and L-Ascorbic acid were purchased from Sigma-Aldrich Co. LLC., Dexamethasone from Adamas-Beta, and TNG $\beta$ 1 was supplied by PeproTech, Inc. Rocky Hills, NJ, USA.

### Experimental layout

To evaluate the *in vivo* stress biomarkers, all the animals were divided into three main groups (i.e. treatment (TP), control (CIA) and normal (NORM)), containing three animals in each group except treatment, which was further divided into two groups illuminated (TP-IL) and non-illuminated (TP-NL) three animals each. The treatment and control comprised of CIA models, whereas normal was kept without CIA and treatment. Similarly, the TP group was subcutaneously injected with TSPP- $\text{TiO}_2$ , whereas control was injected placebo and normal had no CIA and no treatment. One hour post-injection the animals were further exposed to 500-550 nm visible LED light ( $5\text{mW}/\text{dm}^2$  light intensity) for one hour duration with whole body exposure. This light dose is sufficient to achieve the photoactivation through TSPP- $\text{TiO}_2$  nanocomposites. Experiment was continued for two weeks with daily treatment.

The *in vitro* cell culture experiments were performed on primary BMS cells culture obtained from the CIA models. Initially,  $3 \times 10^3$  CIA BMS cells  $\text{ml}^{-1}$  were cultured in six well plates, and after 24 hours various TSPP-TiO<sub>2</sub> concentrations (0, 25, 50, 100  $\mu\text{l}$  of 0.1 mM TSPP + 0.6 mM TiO<sub>2</sub>) were added to BMS cells culture. Then after two hours, one group was exposed to 500-550 nm light for five minutes (i.e., with same intensity as mentioned earlier) and named as TPiL-CIA, whereas the other group was kept non illuminated and named as TPnL-CIA. Similarly, normal BMS cells from healthy rats were obtained and group was named as TPiL-N for illuminated and TPnL-N for non-illuminated TSPP-TiO<sub>2</sub> treatments. Post 72 hours incubation cells were trypsinized and counted by Hemocytometer according to procedure described earlier.<sup>29,30</sup>

### Photosensitizer preparation

The tetra sulphonatophenyl porphyrin (TSPP) was supplied by ABI chemicals and TiO<sub>2</sub> nanowhiskers were generously provided by Dr. Xiao Hua Lu from College of Chemical Engineering, Nanjing University of Technology, Nanjing China. (Fig. 1) TSPP and TiO<sub>2</sub> nanocomposites were separately dissolved in ultrapure deionized water to achieve concentration of 0.1 mM TSPP and 0.6 mM, respectively. TSPP has excellent hydrophilic properties and can readily dissolve in deionized distilled water, whereas TiO<sub>2</sub> readily becomes super hydrophilic when photoactivated<sup>31</sup>. Then TSPP was physically adsorbed on the porous surface of TiO<sub>2</sub> nanowhiskers after mixed in aqueous solution for overnight. The porous nature of TiO<sub>2</sub> nanowhiskers and ionic bonding between the TSPP and TiO<sub>2</sub> provides effective scaffolds for successful delivery and slow release of TSPP from TiO<sub>2</sub> nanowhiskers in desired site. Afterwards, 0.4 ml of TSPP-TiO<sub>2</sub> nanocomposites (0.1 mM TSPP + 0.6 mM TiO<sub>2</sub>) were injected to the TP group. Subsequently, different amount of TSPP-TiO<sub>2</sub> were added to various BMS cells culture for *in vitro* experiments.

### Arthritis models

Collagen Type II and Freund's adjuvant were mixed together by sonication method to form  $1 \text{mg ml}^{-1}$  insoluble emulsion as described earlier<sup>27</sup>. Then immediately within one hour 0.3 ml of emulsion was injected at the base of tail to all animals as subcutaneous parenteral. At day 18 to 21 post injection, all the rats showed obvious clinical signs of CIA. Booster doses were repeated when required.

### BMS cells isolation and culture

The long bones (femur and tibia) were collected from CIA and normal rats. Then by using the cold PBS (pH 7.4) at 4°C with 2% FBS and 1mM EDTA, all the bones were mechanically crushed and bone marrow was obtained for primary cell culture. The bone marrow containing medium was sieved through 70  $\mu\text{m}$  filter and centrifuged at 3000 rpm for 5 minutes to remove the PBS as supernatant. Then the pellet was dispersed and cultured in DMEM/F12 standard medium containing 10% FBS and 1% Penicillin-Streptomycin solution at 37°C temperature, 5% CO<sub>2</sub> and 95% humidity. After three days only sticking cells remained in the tissue culture bottle and non-sticking cells were removed by changing medium and washing with PBS.

### *In vitro* BMS cells proliferation and confirmation

After 72 hours, BMS cells were passaged to 75 cm<sup>2</sup> tissue culture-flasks as passage one and after one week cells were trypsinized (0.25% trypsin) for further experiments. The BMS cells had typical spindle shaped appearance and their plasticity was confirmed by differentiation to chondrocytes and osteocytes as reported earlier<sup>32</sup>. Briefly, cells were trypsinized to 24 well plates as  $5 \times 10^4$  cells well<sup>-1</sup> and incubated for 24 hours to allow cells sticking to the bottom of culture-plate. The standard medium was replaced with Chondrogenic differentiation medium supplemented with L-ascorbic acid 50  $\mu\text{g ml}^{-1}$  and TGF $\beta$ 1 1 ng  $\text{ml}^{-1}$ . Post one week incubation cells were washed with PBS, fixed with 3.7% paraformaldehyde and stained with 0.05% alcian blue stain. For Osteogenic differentiation cells were incubated in standard medium supplemented with ascorbic acid 50  $\mu\text{g ml}^{-1}$ , Na  $\beta$ -glycerphosphate 10 mM and dexamethasone  $10^{-8}$  M for two weeks and then stained with alizarin red 1% after washing and fixation as mentioned earlier<sup>33</sup>. (Fig. 2)

### Serum sampling

Blood samples were collected from all treatment groups via 3 ml 21 gauge needle syringe intracardiac injection, under general anaesthesia of isoflurane<sup>34</sup>. Then the serum was separated by centrifugation at 3000 rpm for 5 minutes and stored at -20°C for further analysis.

### Oxidative stress biomarkers estimation

All antioxidant enzymes and biomarkers were estimated by spectrophotometric methods and the kits were supplied by Nanjing Jiancheng Institute of Bioengineering (Nanjing, Jiangsu, China). The assays were performed according to the manufacturer instructions. The procedure for estimation of CAT, SOD, GPX, TAO and MDA activity was measured by the same procedure as reported earlier<sup>35</sup>. Briefly, the GPX activity was measured as the amount of enzymes that will oxidize the 1  $\mu\text{mol L}^{-1}$  GSH per minute at 37 °C in reaction system for 100  $\mu\text{l}$  of serum. Similarly, the CAT activity was measured by the disappearance rate of  $\text{H}_2\text{O}_2$  at 340 nm in 100  $\mu\text{l}$  serum sample. The SOD activity was measured by the inhibition rate of hydroxylamine oxidation by 50 percent in coupled system using xanthine and xanthine oxidase. The TOA were measured as the reduction of ferric ions by the agent and formation of  $\text{Fe}^{2+}$  TPTZ (2,4,6-tri (2 pyridyl)-s-triazine) blue complex that was treated with phenanthroline for generation of a stable complex the absorption of which was measured at 520 nm. The MDA results were expressed as thiobarbituric acid reactive substance in  $\mu\text{mol } 100^{-1} \mu\text{l}$  of malondialdehyde<sup>36</sup>.

### Statistical analysis

Data were statistically analyzed by SPSS version 18 for analysis of variance (ANOVA) of BMS cells proliferation *in vitro* and t-test was performed for serum biomarkers evaluation. The probability value <0.05 was considered as significant.

## Results

Oxidative species generated by porphyrin derivatives is essential for PDT of any target tissue. In this study we evaluated the effect on the extent of oxidative stress due to the presence of TSPP-TiO<sub>2</sub> nanocomposites for PDT. Subsequently, PDT will lead to drop in oxygen content of the subject system that will influence the BMS cells proliferation rate. Therefore, experiments were performed to find the relationship between the stress enzymes mean during PDT with TSPP combined with TiO<sub>2</sub> nanowhiskers and the growth rate of BMS cells from the RA infected murine models.

### *In vivo* stress biomarkers

The TSPP-TiO<sub>2</sub> nanocomposites have been successfully used to ameliorate the RA during PDT after evaluating their protective effect on the circulatory and excretory

system in the *in vivo* murine experimental models<sup>27,28</sup>. Since in PDT, the PS generates ROS and <sup>1</sup>O<sub>2</sub> for ablation of tumor or amelioration of other diseases, the relevant stress biomarkers could be further explored in other than targeted tissues. Therefore, the stress biomarkers mean values were estimated from the blood serum after TSPP-TiO<sub>2</sub> photoactivation and values expressed are the mean values per 100  $\mu\text{l}$  of various groups.

All the mean values for CAT, SOD, GR, GPX, and MDA were significantly ( $p < 0.01$ ) affected by the TSPP-TiO<sub>2</sub> either illuminated or dark, whereas the value of total antioxidants remained non-significant with probability value more than 0.05.

The CAT mean value in CIA was  $11.72 \pm 0.75$  (SD) U/100  $\mu\text{l}$ , which was lower than TP-NL ( $13.08 \pm 1.70$ ) and TP-L ( $13.35 \pm 1.26$ ), whereas in normal group its mean remained  $14.39 \pm 1.53$  (SD) U/100  $\mu\text{l}$  (Fig. 3a). Similarly, the SOD mean value was higher in TP-L ( $127.74 \pm 4.5$  (SD) U/100  $\mu\text{l}$ ), followed by TP-NL ( $118.11 \pm 7.87$  (SD) U/100  $\mu\text{l}$ ) and CIA ( $112.77 \pm 2.43$  (SD) U/100  $\mu\text{l}$ ), whereas the normal group value was highest i.e.  $137.44 \pm 3.45$  (SD) U/100  $\mu\text{l}$ . (Fig. 3d)

The mean value of GPX observed in TP-L ( $157.90 \pm 5.15$ ) was highest among the CIA and TP-NL was  $154.03 \pm 3.74$  (SD) U/100  $\mu\text{l}$  and  $149.714474 \pm 7.34$  (SD) U/100  $\mu\text{l}$ , respectively, whereas the normal group serum GPX value was  $192.89 \pm 11.52$  (SD) U/100  $\mu\text{l}$  (Fig 3b). The GR serum mean value remained almost the same among all treated groups of CIA, TP-L and TP-NL, i.e.,  $17.904100 \pm 1.48$ ,  $17.71 \pm 2.16$ ,  $17.71 \pm 2.167$  (SD) U/100  $\mu\text{l}$  respectively, whereas the normal rats serum value estimate for GR was  $25.63 \pm 1.56$  (SD) U/100  $\mu\text{l}$ . Moreover, the lowest TAO level was observed in the TP-L group ( $9.78 \pm 1.60$  (SD) U/100  $\mu\text{l}$ ) as compared to the CIA ( $13.06 \pm 1.69$  (SD) U/100  $\mu\text{l}$ ), TP-NL ( $13.29 \pm 2.13$  (SD) U/100  $\mu\text{l}$ ) and normal group ( $12.15 \pm 1.85$  (SD) U/100  $\mu\text{l}$ ). (Fig. 3a) The MDA mean concentration value was lowest in TP-L ( $123.88 \pm 10.41$  (SD) U/100  $\mu\text{l}$ ) among treated groups, i.e. TP-NL ( $169.41 \pm 6.09$  (SD) U/100  $\mu\text{l}$ ) and CIA ( $143.31 \pm 9.97$  (SD) U/100  $\mu\text{l}$ ), respectively, and the normal group mean serum concentration was  $75.06 \pm 7.68$  (SD) U/100  $\mu\text{l}$  (Fig. 3c).

### *In vitro* BMS cells growth effect

The BMS cells proliferation was significantly affected by various concentrations of TSPP-TiO<sub>2</sub> ( $p < 0.01$ ) and illumination ( $p < 0.05$ ). Similarly, the proliferation rate

of BMS cells was also significantly ( $p < 0.01$ ) affected by the CIA, as compared to normal BMS cells count mean.

In the post treatment highest cell number mean  $\pm$  standard deviation (SD) was observed in 25  $\mu$ l TPiL-BMS cells group ( $12.33 \times 10^6 \pm 2.72$  (SD)), that is 33.79 % higher as compared to TPnL-BMS cells, i.e.,  $8.17 \times 10^6 \pm 1.17$  (SD). The cell count mean for 50  $\mu$ l, 100  $\mu$ l and control group concentration of nanocomposites TSPP-TiO<sub>2</sub> treatment was  $8.8 \times 10^6 \pm 2.37$  (SD),  $5.67 \times 10^6 \pm 0.57$  (SD),  $9.33 \times 10^6 \pm 3.93$  (SD), respectively, in comparison with TPiL-BMS cells group, i.e.,  $7.2 \times 10^6 \pm 2.16$  (SD),  $5 \times 10^6 \pm 1.73$  (SD),  $6.67 \times 10^6 \pm 0.57$  (SD), respectively. The percent change in cell proliferation was 18.2, 11.7 and 28.5% in 50  $\mu$ l, 100  $\mu$ l and control group, respectively. (Fig. 4)

The illumination effect on mean in normal BMS cells was  $3 \times 10^6 \pm 1.67$  (SD),  $1.17 \times 10^6 \pm 1.0$  (SD),  $3 \times 10^6 \pm 3.4$  (SD),  $6.67 \times 10^6 \pm 3.7$  (SD) for 25, 50, 100  $\mu$ l of nanocomposites TSPP-TiO<sub>2</sub> treatment and control group, respectively; whereas  $2.60 \times 10^6 \pm 1.7$  (SD),  $2.67 \times 10^6 \pm 1.3$  (SD),  $2 \times 10^6 \pm 1.0$  (SD),  $4 \times 10^6 \pm 1.0$  (SD), respectively, was mean count in TPnL-N group.

## Discussion

PDT is considered one of the most efficient therapy for many superficial malignant and benign tumors, in addition to other microbial infections<sup>37</sup>. PDT has been more extensively used to induce apoptosis or necrosis in neoplastic tissues; however, in some cases like Hypericin PDT has been reported to coincide with growth enhancement effect on human neoplasms<sup>38</sup>. Similarly, Aluminum-Phthalocyanin mediated PDT has also been associated with growth promoting effect on osteoblast cells<sup>39</sup>. The role of PDT is of interest in cures of autoimmune diseases especially RA<sup>40</sup>. In previous studies we reported a new therapeutic effect of photoactivated TSPP-TiO<sub>2</sub> nanocomposites on RA<sup>27, 28</sup>. This discovery led us to the new domain in theranostics; therefore we extended its potential applications to the BMS cells in the CIA infected models and evaluated the stress enzymes profile as oxidative stress biomarkers in TSPP-TiO<sub>2</sub> nanocomposites treated animal models.

During PDT the ROS and <sup>1</sup>O<sub>2</sub> are generated from the photoactivated nanocomposite TSPP-TiO<sub>2</sub> in the presence biologically available molecular oxygen. These ROS and <sup>1</sup>O<sub>2</sub> will interfere with cellular signal pathways; meanwhile, the cell in response will neutralize these

ROS by activating intra and inter-cellular anti oxidative cellular enzymes system<sup>41</sup>. ROS play a vital role in intra and inter-cellular signaling. However, the uncontrolled generation of ROS will disturb the oxidative and anti-oxidative equilibrium in the cell and lead to lipid peroxidation that is directly proportional to cellular SOD, GPX, CAT, GR and inversely proportional to the MDA level<sup>22</sup>. Moreover, the oxidative enzyme activity is lowered due to inhibitory effect of nanocomposites on mRNA expression of these enzymes<sup>22</sup>. The disturbance of the ROS equilibrium within the cell is referred to as oxidative stress which leads to oxidation of DNA, and degradation of cellular organelles, proteins and lipids<sup>21</sup>.

Porphyrin derivatives are well known for oxidative stress during PDT<sup>15, 42</sup>, although when TSPP was combined with TiO<sub>2</sub> nanowhiskers, the oxidative stress effect was mitigated<sup>28</sup>. This may do due to the fact that TSPP is adsorbed in the pores of TiO<sub>2</sub> nanowhiskers and released slowly during a long time period. The <sup>1</sup>O<sub>2</sub> quantum yield  $\Phi^{\Delta}$  value for only TSPP was earlier reported as 0.64<sup>43</sup>, while we determined a somewhat lower value of 0.44<sup>27</sup> for the nanocomposite material TSPP:TiO<sub>2</sub> with a ratio of 1:2 (by mass). This quantum yield is still sufficiently high for PDT, consistent with our results presented in this paper. Moreover, the size and type of nano titania also affect the cellular anti-oxidative enzymes, i.e., nano TiO<sub>2</sub> with smaller size are more cytotoxic than larger size, similarly, TiO<sub>2</sub> nanoparticles are reported more cytotoxic than TiO<sub>2</sub> nanowhiskers<sup>44</sup>. In our earlier study the MTT assay results also revealed that when TSPP was combined with TiO<sub>2</sub> nanowhiskers, the cell viability remained 100% and 80% in lower and higher concentration of TSPP-TiO<sub>2</sub> nanocomposites, respectively, as compared to the TSPP alone, i.e., less than 70%<sup>28</sup>.

Our results showed a higher level of SOD when TSPP-TiO<sub>2</sub> nanocomposites were photoactivated *in vivo*, while the CAT level remained almost same as dark TSPP-TiO<sub>2</sub> nanocomposites and control group. H<sub>2</sub>O<sub>2</sub> has potential to penetrate cell membranes and can lead to lipid peroxidation. Generally, SOD, GPX and CAT neutralize H<sub>2</sub>O<sub>2</sub> to stable alcohols and water to avoid damage to biomolecules<sup>45</sup>. Additionally, almost the same concentration mean of CAT in nanocomposites TSPP-TiO<sub>2</sub> treated groups vouches its inertness to the normal body cells. Moreover, the highest level of GR also demonstrates the least ROS generation from the photoactivated TSPP-TiO<sub>2</sub> nanocomposites. The

primary role of GR is to reduce the oxidized glutathione by the help of NADPH<sup>21</sup>.

The MDA is a major product of lipid peroxidation and used as prototype biomarker for cell membrane oxidative damage<sup>46</sup>. The MDA least mean was observed in photoactivated nanocomposites TSPP-TiO<sub>2</sub> groups. The lower MDA level shows a protective effect of TSPP-TiO<sub>2</sub> nanocomposites on lipid peroxidation. Our results are in contrast with findings reported in the literature due to the fact that the previous studies used single and pristine TiO<sub>2</sub> nanoparticles only in the brain, which are known to be more cytotoxic<sup>22, 47</sup>. We used TiO<sub>2</sub> nanowhiskers, which were reported to be safer than nanoparticles<sup>48</sup> and also combined these whiskers with TSPP to evaluate their stress on the whole body system. Nevertheless, Porphyrin in combination with Mn (iii) (MnTM-2-PyP<sup>5+</sup>) has been reported by Benov and Batinic-haberle for lowering the overall MDA level in streptozotocin diabetic rats<sup>49</sup>. Their results are in agreement with our findings.

TAO is the measure of estimated antioxidant capacity of the body and its lower value is indicator of overall oxidative stress<sup>35</sup>. Generally, the TAO estimates the chain-breaking antioxidants in liquid (thiols, urates, bilirubin, and ascorbate) and lipid phase (flavonoids,  $\alpha$ -tocopherol, and carotenoids)<sup>50</sup>. We found almost the same TAO mean value in all treated groups, which indicate the safety of TSPP-TiO<sub>2</sub> nanocomposites.

CIA BMS cells proliferation rate was found surprisingly higher in photoactivated TSPP-TiO<sub>2</sub> nanowhiskers treated group. In RA, the synovial milieu has unique pathophysiological environment, i.e., hypoxia and comprised of various stress enzymes and biomarkers<sup>51, 52</sup>. Jimenez-Boj et al reported that Rheumatoid joint tissue gets bilateral insult, i.e., inflammation in the synovial milieu, and elevated pro-inflammatory cytokines activities and inflammatory (T&B) cells aggregates inside the bone marrow<sup>53</sup>. Therefore, we can also assume that hypoxic condition exist inside the bone marrow. Since PDT utilizes biologically available oxygen to generate ROS<sup>54</sup>, this will lead to a further drop in oxygen concentration and relatively higher stress enzyme level may have some beneficial effect on the growth rate of CIA BMS cells. Moreover, it has already been proven that lower oxygen level promotes growth rate of hematopoietic stem cells<sup>55</sup>, neural crest cells<sup>56</sup> and survival of embryonic stem cells<sup>57</sup>. Similarly, Yamanaka et al. also reported that hypoxic conditions

(5%) promote the growth rate in induced pluripotent stem cells<sup>58</sup>.

It has been proven that during PDT the bioavailable oxygen at ground state is photochemically consumed by PS to generate <sup>1</sup>O<sub>2</sub><sup>15</sup>. This will result in rapid reduction of oxygen bioavailability in the subject tissue as reported earlier<sup>59, 60</sup>. Therefore, the TSPP-TiO<sub>2</sub> nanocomposites PDT provides scaffolds for the hypoxic environment by utilizing biologically available oxygen to generate ROS and <sup>1</sup>O<sub>2</sub> in the rheumatoid joint milieu and bone marrow in the vicinity, which is helpful for BMS cells proliferation to cope with RA either by tissue repair<sup>61</sup> or by suppressing the autoimmunity<sup>62</sup>.

## Conclusion

In summary, from the above results we conclude that the photoactivated TSPP-TiO<sub>2</sub> nanocomposites are safer in terms of anti-oxidative biomarkers during RA PDT, and can be used for biomedical applications. Moreover, in CIA the ex vivo BMS cells treated with photoactivated TSPP-TiO<sub>2</sub> nanocomposites can increase the proliferation rate, which is helpful in lowering the autoimmune reactions and ameliorate tissue injury.

## Acknowledgements

This work is supported by the National Natural Science Foundation of China (Grant 81325011), National High Technology Research & Development Program of China (Grants 2015AA020502 and 2012AA022703), and Major Science & Technology Project of Suzhou (Grant ZXY2012028). M.S. acknowledges support from the NSF-CREST program (NSF Grant HRD-0932421). The authors are also thankful to Dr. Hussain Ahmad for help in stress biomarkers evaluation experiments.

## Notes and references

1. A. I. Caplan, *J Orthopaed Res*, 1991, **9**, 641-650.
2. J. E. Grove, E. Bruscia and D. S. Krause, *Stem Cells*, 2004, **22**, 487-500.
3. A. Friedenstein, R. Chailakhyan and U. Gerasimov, *Cell Proliferat*, 1987, **20**, 263-272.
4. A. Corcione, F. Benvenuto, E. Ferretti, D. Giunti, V. Cappiello, F. Cazzanti, M. Risso, F. Gualandi, G. L. Mancardi and V. Pistoia, *Blood*, 2006, **107**, 367-372.
5. O. Lindvall, Z. Kokaia and A. Martinez-Serrano, *Nat Med*, 2004, **10**, S42-S50.

6. G. M. Zou, *J Cell Physiol*, 2007, **213**, 440-444.
7. B. T. Himes, B. Neuhuber, C. Coleman, R. Kushner, S. A. Swanger, G. C. Kopen, J. Wagner, J. S. Shumsky and I. Fischer, *Neurorehab Neural Re*, 2006, **20**, 278-296.
8. A. Bacigalupo, M. Valle, M. Podestà, A. Pitto, E. Zocchi, A. De Flora, S. Pozzi, S. Luchetti, F. Frassoni and M. T. Van Lint, *Exp Hematol*, 2005, **33**, 819-827.
9. M. F. Clarke, J. E. Dick, P. B. Dirks, C. J. Eaves, C. H. Jamieson, D. L. Jones, J. Visvader, I. L. Weissman and G. M. Wahl, *Cancer Res*, 2006, **66**, 9339-9344.
10. G. S. Firestein, *Nature*, 2003, **423**, 356-361.
11. L. Klareskog, L. Padyukov and L. Alfredsson, *Curr Opin Rheumatol*, 2007, **19**, 49-54.
12. A. A. Schuna, *Journal of the American Pharmaceutical Association (Washington, DC: 1996)*, 1997, **38**, 728-735; quiz 735-727.
13. I. B. McInnes and G. Schett, *Nat Rev Immunol*, 2007, **7**, 429-442.
14. L. Chen, B. Bao, N. Wang, J. Xie and W. Wu, *Pharmaceuticals*, 2012, **5**, 339-352.
15. T. J. Dougherty, C. J. Gomer, B. W. Henderson, G. Jori, D. Kessel, M. Korbelik, J. Moan and Q. Peng, *J Natl Cancer Inst*, 1998, **90**, 889-905.
16. R.-M. Ion, *Current Topics in Biophysics*, 2000, **24**, 21-34.
17. L. B. Josefsen and R. W. Boyle, *Theranostics*, 2012, **2**, 916-966.
18. L. Guyon, M.-O. Farine, J. C. Lesage, A.-M. Gevaert, S. Simonin, C. Schmitt, P. Collinet and S. Mordon, *Photodiagn Photodyn*, 2014, **11**, 265-274.
19. D. Daicoviciu, A. Filip, R. M. Ion, S. Clichici, N. Decea and A. Muresan, *Folia Biol (Praha)*, 2011, **57**, 12-19.
20. A. L. N. Francisco, W. R. Correr, L. H. Azevedo, V. G. Kern, C. A. L. Pinto, L. P. Kowalski and C. Kurachi, *Photodiagn Photodyn*, 2014, **11**, 82-90.
21. J. Nordberg and E. S. Arner, *Free Radical Bio Med*, 2001, **31**, 1287-1312.
22. L. Ma, J. Liu, N. Li, J. Wang, Y. Duan, J. Yan, H. Liu, H. Wang and F. Hong, *Biomaterials*, 2010, **31**, 99-105.
23. T. Rajh, N. M. Dimitrijevic, M. Bissonnette, T. Koritarov and V. Konda, *Chem Rev*, 2014, **114**, 10177-10216.
24. F. Rehman, C. Zhao, H. Jiang and X. Wang, *Biomater Sci*, 2015.
25. R. Cai, K. Hashimoto, K. Itoh, Y. Kubota and A. Fujishima, *B Chem Soc Jpn*, 1991, **64**, 1268-1273.
26. Q. Li, X. Wang, X. Lu, H. Tian, H. Jiang, G. Lv, D. Guo, C. Wu and B. Chen, *Biomaterials*, 2009, **30**, 4708-4715.
27. C. Zhao, F. U. Rehman, Y. Yang, X. Li, D. Zhang, H. Jiang, M. Selke, X. Wang and C. Liu, *Sci Rep*, 2015, **5**, 11518.
28. F. U. Rehman, C. Zhao, H. Jiang, M. Selke and X. Wang, *Photodiagn Photodyn*, 2015, DOI: 10.1016/j.pdpdt.2015.08.005.
29. O. Bastidas, *Celeromics*, 2013.
30. I. Sekiya, B. L. Larson, J. R. Smith, R. Pochampally, J. G. Cui and D. J. Prockop, *Stem Cells*, 2002, **20**, 530-541.
31. X. Chen and S. S. Mao, *Chem Rev*, 2007, **107**, 2891-2959.
32. M. Dominici, K. Le Blanc, I. Mueller, I. Slaper-Cortenbach, F. Marini, D. Krause, R. Deans, A. Keating, D. Prockop and E. Horwitz, *Cytotherapy*, 2006, **8**, 315-317.
33. A. Augello, R. Tasso, S. M. Negrini, A. Amateis, F. Indiveri, R. Cancedda and G. Pennesi, *Eur J Immunol*, 2005, **35**, 1482-1490.
34. S. Parasuraman, R. Raveendran and R. Kesavan, *J Pharmacol Pharmacother*, 2010, **1**, 87-93.
35. H. Ahmad, J. Tian, J. Wang, M. A. Khan, Y. Wang, L. Zhang and T. Wang, *J Agr Food Chem*, 2012, **60**, 7111-7120.
36. J. A. Buege and S. D. Aust, *Method Enzymol*, 1978, **52**, 302-310.
37. Z. Chu, S. Zhang, C. Yin, G. Lin and Q. Li, *Biomater Sci*, 2014, **2**, 827-832.
38. R. Ackroyd, C. Kelty, N. Brown and M. Reed, *Photochem Photobiol*, 2001, **74**, 656-669.
39. S. Y. Vasilchenko, A. I. Volkova, A. V. Ryabova, V. B. Loschenov, V. I. Konov, A. A. Mamedov, S. G. Kuzmin and E. A. Lukyanets, *J Biophotonics*, 2010, **3**, 336-346.
40. J. Neupane, S. Ghimire, S. Shakya, L. Chaudhary and V. P. Shrivastava, *Photodiagn Photodyn*, 2010, **7**, 44-49.
41. H. Sies, *Exp Physiol*, 1997, **82**, 291-295.
42. C. J. Gomer, A. Ferrario, N. Rucker, S. Wong and A. S. Lee, *Cancer Res*, 1991, **51**, 6574-6579.
43. J. Davila and A. Harriman, *Photochem Photobiol*, 1990, **51**, 9-19.
44. J. Zhao, L. Bowman, X. Zhang, V. Vallyathan, S.-H. Young, V. Castranova and M. Ding, *J Toxicol Env Heal A*, 2009, **72**, 1141-1149.



45. D. Drobne, A. Jemec and Ž. P. Tkalec, *Environ Pollut*, 2009, **157**, 1157-1164.
46. M. Scott, J. Van den Berg, T. Repka, P. Rouyer-Fessard, R. Hebbel, Y. Beuzard and B. Lubin, *J Clin Invest*, 1993, **91**, 1706.
47. B. L. Baisch, N. M. Corson, P. Wade-Mercer, R. Gelein, A. J. Kennell, G. Oberdorster and A. Elder, *Part Fibre Toxicol*, 2014, **11**, 5.
48. N. Wu, J. Wang, D. N. Tafen, H. Wang, J.-G. Zheng, J. P. Lewis, X. Liu, S. S. Leonard and A. Manivannan, *J Am Chem Soc*, 2010, **132**, 6679-6685.
49. L. Benov and I. Batinic-Haberle, *Free Radical Res*, 2005, **39**, 81-88.
50. D. Koracevic, G. Koracevic, V. Djordjevic, S. Andrejevic and V. Cosic, *J Clin Pathol*, 2001, **54**, 356-361.
51. R. Maini and P. Taylor, *Annu Rev Med*, 2000, **51**, 207-229.
52. I. B. McInnes and F. Y. Liew, *Nat Clin Pract Rheum*, 2005, **1**, 31-39.
53. E. Jimenez-Boj, K. Redlich, B. Türk, B. Hanslik-Schnabel, A. Wanivenhaus, A. Chott, J. S. Smolen and G. Schett, *The Journal of Immunology*, 2005, **175**, 2579-2588.
54. K. Sato, T. Nakajima, P. L. Choyke and H. Kobayashi, *RSC advances*, 2015, **5**, 25105-25114.
55. G. H. Danet, Y. Pan, J. L. Luongo, D. A. Bonnet and M. C. Simon, *J Clin Invest*, 2003, **112**, 126.
56. S. J. Morrison, M. Csete, A. K. Groves, W. Melega, B. Wold and D. J. Anderson, *The Journal of Neuroscience*, 2000, **20**, 7370-7376.
57. T. Ezashi, P. Das and R. M. Roberts, *P Natl Acad Sci Usa*, 2005, **102**, 4783-4788.
58. Y. Yoshida, K. Takahashi, K. Okita, T. Ichisaka and S. Yamanaka, *Cell Stem Cell*, 2009, **5**, 237-241.
59. J. Zilberstein, A. Bromberg, A. Frantz, V. Rosenbach - Belkin, A. Kritzman, R. Pfefermann, Y. Salomon and A. Scherz, *Photochem Photobiol*, 1997, **65**, 1012-1019.
60. B. Tromberg, A. Orenstein, S. Kimel, S. Barker, J. Hyatt, J. Nelson and M. Berns, *Photochem Photobiol*, 1990, **52**, 375-385.
61. N. Goonoo, A. Bhaw-Luximon and D. Jhurry, *RSC Advances*, 2014, **4**, 31618-31642.
62. C. Bocelli-Tyndall, L. Bracci, G. Spagnoli, A. Braccini, M. Bouchenaki, R. Ceredig, V. Pistoia, I. Martin and A. Tyndall, *Rheumatology*, 2007, **46**, 403-408.

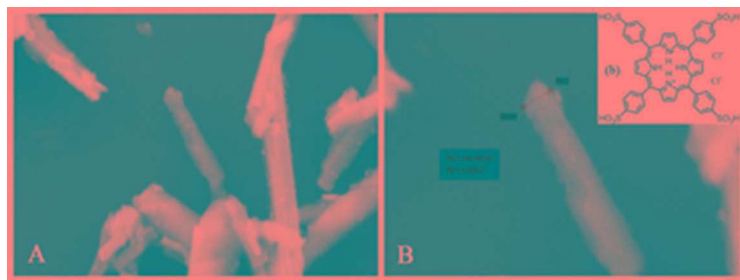
**Scheme 1** Bone Marrow Stem Cells isolation and in vitro proliferation from collagen induced arthritis murine models

**Fig. 1** SEM micrograph of TiO<sub>2</sub> nanowhiskers (A), average size (B) and Tetra Sulphonatophenyl Porphyrin structural formula (b) (scale 200 nm)

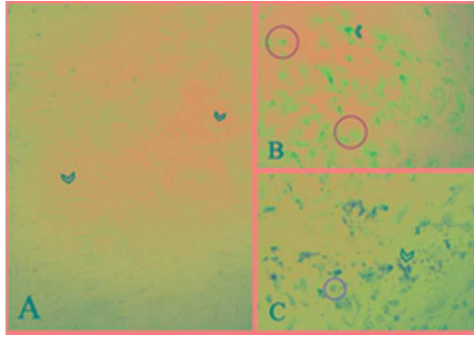
**Fig. 2** Collagen induced arthritis Bone Marrow Stem Cells; black arrow head clearly demonstrate characteristic typical spindle shaped cells (A), Cells differentiated to Chondrocytes (red circles) and arrow head shows cartilaginous beads (arrow head) (B) and typical osteoblast (in red circles) with mineral deposition (arrow heads) (C).

**Fig. 3 (a)** Showing blood serum level of CAT (black line), GR (red line) and TAO (yellow line); **(b)** GPX mean value; **(c)** MDA level and **(d)** is demonstrating SOD in treatment group CIA (collagen induced arthritis) as control, TP-NL (TSPP-TiO<sub>2</sub> group without illumination), TP-L (TSPP-TiO<sub>2</sub> illuminated) and Normal group. Whereas, CAT stand for catalase, GR for glutathione reductase, TAO for Total Anti-Oxidant Count, GPX for glutathione peroxidase, MDA for malondialdehyde and SOD for Super Oxide Dismutase. For all oxidative stress bio-markers probability value was < 0.01 except TAO (p > 0.05)

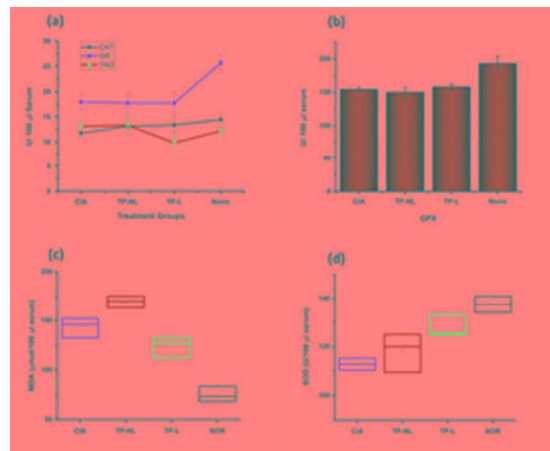
**Fig. 4** Collagen induced arthritis rat bone marrow stem cells proliferation rate in vitro after treatment with various concentrations of Tetra Sulphonatophenyl Porphyrin and TiO<sub>2</sub> nanocomposites illuminated and dark. (p < 0.01)



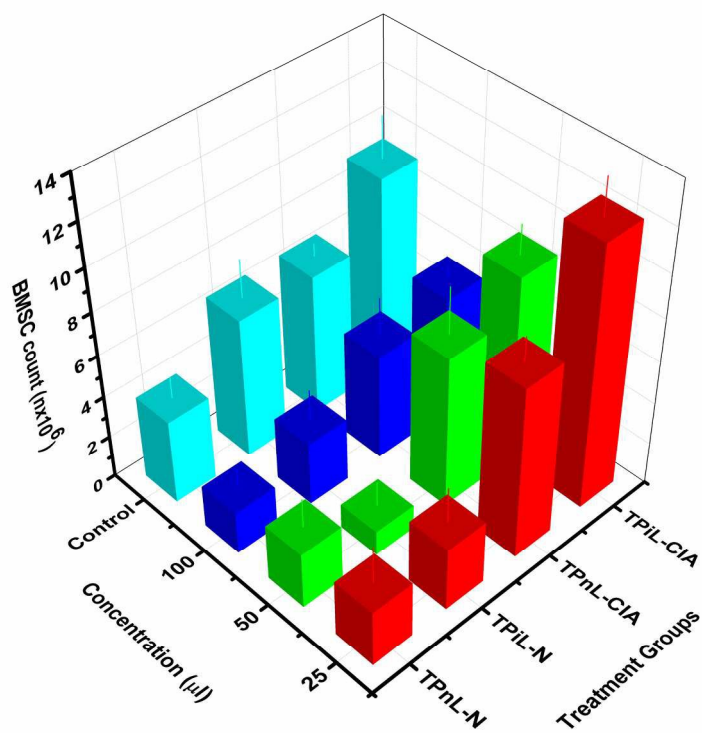
31x11mm (300 x 300 DPI)



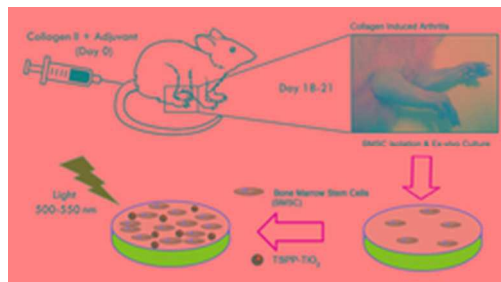
20x14mm (300 x 300 DPI)



23x18mm (300 x 300 DPI)



208x159mm (300 x 300 DPI)



21x11mm (300 x 300 DPI)